

Article

# Design, synthesis and application of pyrazole-based Schiff base chitosan hybrids for Cu(II) removal and antibacterial inhibition

Reham A. Abdel-Monem\*, Samira T. Rabie, Yasser M. A. Mohamed, Hossam A. El Nazer

Photochemistry Department, National Research Centre, Dokki, Giza 12622, Egypt

\* Corresponding author: Reham A. Abdel-Monem, [rehamakram2007@gmail.com](mailto:rehamakram2007@gmail.com)

## CITATION

Abdel-Monem RA, Rabie ST, Mohamed YMA, El Nazer HA. Design, synthesis and application of pyrazole-based Schiff base chitosan hybrids for Cu(II) removal and antibacterial inhibition. *Journal of Polymer Science and Engineering*. 2025; 8(1): 11536. <https://doi.org/10.24294/jpse11536>

## ARTICLE INFO

Received: 23 February 2025

Accepted: 8 May 2025

Available online: 26 June 2025

## COPYRIGHT



Copyright © 2025 by author(s).

*Journal of Polymer Science and Engineering* is published by EnPress Publisher, LLC. This work is licensed under the Creative Commons Attribution (CC BY) license. <https://creativecommons.org/licenses/by/4.0/>

**Abstract:** Modified chitosan hybrids were obtained via chemical reaction of chitosan with two pyrazole aldehyde derivatives to produce two chitosan Schiff bases, Cs-SB1, and Cs-SB2, respectively. FTIR spectroscopy and scanning electron microscopy confirmed both chemical structures and morphology of these Schiff bases. Thermal gravimetric analysis showed an improvement of thermal properties of these Schiff bases. Both chitosan Schiff bases were evaluated in a batch adsorption approach for their ability to remove Cu(II) ions from aqueous solutions. Energy dispersive X-ray for the Schiff bases adsorbed metal ions in various aqueous solutions was performed to confirm the existence of adsorbed metal ions on the surface substrate and their adsorptive efficiency for Cu(II) ions. Results of the batch adsorption method showed that prepared Schiff bases have good ability to remove Cu(II) ions from aqueous solutions. The Langmuir isotherm equation showed a better fit for both adsorbents with regression coefficients ( $R^2 = 0.97$  and  $0.99$ , respectively) with maximum adsorption capacity for Cu(II) of 10.33 and 39.84 mg/g for Cs-SB1 and Cs-SB2, respectively. All prepared compounds, pyrazoles and two chitosan Schiff bases, showed good antimicrobial activity against three Gram +ve bacteria, three Gram -ve bacteria and *Candida albicans*, with varying degrees when compared to the standard antimicrobial agents.

**Keywords:** pyrazole-chitosan Schiff bases; Cu(II) ions; batch adsorption method; antimicrobial activity

## 1. Introduction

Accumulation of heavy metal in ecological communities is considered to be a global issue. Both human health and the natural system are threatened by the accumulated heavy metals in drinking water. Environmental pollutants by heavy metals are considered to be one of the most important issues [1]. Release of heavy metals into the environment may also result via volcanic eruptions and the weathering of rocks [2,3]. The harmful effects of most heavy metals on living organisms are observed when their concentrations exceed the environmentally permitted limits. These pollutants can be absorbed by marine organisms and are not biodegradable. Heavy metals have a tendency to accumulate in living tissues, causing disruption of the human body once their concentrations reach a level where they can penetrate the food chain [4]. Industrial wastewater-related transition metal poisoning is an important problem. Transition metal ions are released in different amounts by a wide range of applications as the mining, metallurgical, electroplating pigment, and leather industries. Zinc, cadmium, chromium, copper, lead, manganese, and iron are the most common metal ions found in both natural and industrial effluent [5]. Copper organic complexes with strong chemical stability and high solubility in water are difficult to eliminate with traditional adsorbents. A novel

amidoxime nanofiber (AO-Nanofiber) with the  $p$ - $\pi$  conjugated structure was fabricated through homogeneous chemical grafting coupled with electrospinning and applied to capture cupric tartrate (Cu-TA) from aqueous solutions [6]. Some studies were performed on the removal of palladium metal ions via nanofibers modified by 8-hydroxyquinoline [7] and by 2-Thionicotinic acid [8]. Hence, to protect both public health and the environment, it is crucial to reduce the presence of certain heavy metals in water sources. Chitosan polymers are considered to be semi-artificial amino polysaccharides with significant structural features, very contemporary applicability, and used on a large scale in biomedical industrial fields [9]. Chitosan is a naturally occurring bioactive polymer that is freely available, nontoxic, edible, renewable, natural, and biodegradable and has the property of biocompatibility [10]. Chitosan exhibits many advantageous biological properties, such as hemostatic, anticancer, and antimicrobial activities, that facilitate wound healing [11]. It is also applied in various industrial fields as water purification, plant security, drug delivery, restorative materials and metal particle chelation [12–14]. Chitosan is regarded as a good natural adsorbent for Cu, Ni, Cr, Zn, and Pb metal ions. These factors may be due to the presence of both hydroxyls and primary amino groups, which are thought to be sorption sites, as well as the flexible chain structure of the polymer, which serves as an appropriate supplier for the complexity of metal ions [15]. Many publications have been conducted on chelating polymers based on chitosan. It demonstrated the improved sorption capabilities for the intended ions in either single or mixed solutions as well as the higher stability or reusability of the innovative chitosan-based resins [16–18]. The reactive amino groups are utilized to carry out a number of reactions. One of these examples is the reductive amination process that resulted in a chemical reaction between aldehydes and the amino groups of chitosan [19]. The Schiff bases produced from this chemical reaction are an important class of ligands that can chelate some metal ions via their azomethine nitrogen atom [20]. The C=N bond in azomethine derivatives is important since some of these derivatives are found to have significant biological activities [21]. Schiff bases are used in wide and various applications as catalysis, analytical chemistry, fungicidal and agrochemical, in addition to both food and dye industries [22,23]. The prevalence of deep mycosis needs a greater focus on finding new, more potent antimicrobial medications with fewer side effects. Schiff bases and their metal complexes are known as remarkable stereochemical models in coordination chemistry of the main group and transition metals because of readily available preparation methods and structural diversity [24]. There are some Schiff base-functionalized siloxanes that have been discovered as promising candidates for decreasing toxic metal concentrations in water [25,26]. On the other hand, these materials and their complexes have also generated an interest in homogeneous catalysis [27]. It was determined that the most significant chitosan derivatives were produced through chemical reaction of Schiff bases because modified chitosan exhibited exceptional properties and they were used in both pharmacological and medicinal application fields [28,29]. In 2022, it was investigated that some newly prepared aldehydes were reacted with chitosan to obtain chitosan-Schiff-base derivatives that were subsequently utilized as adsorbents for metal ions such as Zn(II), Cu(II), and Cr(III) [30]. In addition, it was demonstrated that chitosan has

reacted with salicylaldehyde and some of its derivatives in aqueous solutions to afford chitosan Schiff base derivatives that act as adsorbents for Cu(II) ions [31]. Moreover, chitosan-Schiff-base compounds showed a wide range of uses as biocides [32], in coordination chemistry as well as metal chelating agents [33]. It was reported that many attempts to produce chitosan-Schiff bases by its modification with the aldehyde moiety of pyrazole carbaldehyde to achieve improved antimicrobial activity. Different pyrazole derivatives were applied to perform a series of Schiff bases of chitosan [34]. Many compounds with pyrazole moiety have shown strong antimicrobial, anticancer, and antioxidant activities [35–37]. This work aims to prepare new pyrazole-based aldehydes containing two different aromatic rings to react with chitosan since the formed chitosan-Schiff bases can be utilized in the adsorption of Cu(II) metal ions from aqueous solutions. Performance of a series of batch adsorption experiments under various experimental conditions as pH, initial concentration of Cu and adsorbent mass. Evaluation of antimicrobial activities of all prepared compounds against some types of microorganisms was also carried out.

## **2. Experimental**

### **2.1. Materials**

Chitosan (MW 100–300 kDa 82% degree of deacetylation) was purchased from Across Organics, Belgium. Potassium persulfate (KPS),  $\text{CuCl}_2 \cdot 2\text{H}_2\text{O}$ . All other chemicals were of fine grades and all solvents were distilled before use.

### **2.2. Characterization techniques and analysis**

#### **2.2.1. Fourier transform infrared (FTIR) spectroscopy**

FTIR spectra were recorded on a Shimadzu IR-spectrometer (FTIR 8201) Japan, at room temperature within the wavenumber range of 4000 to 400  $\text{cm}^{-1}$  using KBr discs.

#### **2.2.2. Thermogravimetric analysis (TGA)**

Thermogravimetric analysis was carried out on a TGA-50H thermogravimetric analyzer, Shimadzu, Japan. Samples were heated from 50 up to 800 °C in a platinum pan with a heating rate of 10 °C/min, in  $\text{N}_2$  atmosphere of flow rate 25 mL/min.

#### **2.2.3. Scanning electronic microscopy (SEM)**

The dry samples were spread on a conducting adhesive tape, pasted on a metallic stub. The morphologies of the tested samples were investigated and imaged with a scanning electron microscope (SEM) (QUANTA FEG 250 ESEM, USA). This was accompanied by energy dispersive X-ray spectroscopy (EDAX AMETEK Inc.; Mahwah, NJ, USA) at an acceleration voltage of 15 kV. The films were fixed on the surface of a sticky tape.

### **2.3. Preparation of hydrazine derivatives**

Two derivatives of hydrazine were prepared by the reaction of hydrazine hydrate with 4-methoxy acetophenone, acetyl thiophene (in separate) taking equimolar ratios of each in glacial acetic acid and refluxing for 6 h. The reaction

mixture was then treated with diethyl ether and left overnight to collect the white solid product affording the hydrazine derivatives.

#### 2.4. Preparation of pyrazole-aldehyde derivatives

Hydrazine derivative (1.0 mol) was added to 2.0 moles of dimethylformamide and phosphorus oxychloride (DMF-POCl<sub>3</sub>) and left overnight at room temperature. KOH/methanol solution (10%) was added to the reaction mixture that was refluxed for 3 h and left to cool producing two pyrazole aldehyde derivatives [38]. The two afforded derivatives named, 3-(4-methoxyphenyl)-4-methelene-1H-pyrazole and 4-methelene-3-(thiophen-2-yl)-1H-pyrazole with codes Pz1 and Pz2, respectively, are represented in Scheme 1 (See **Figure 1**).

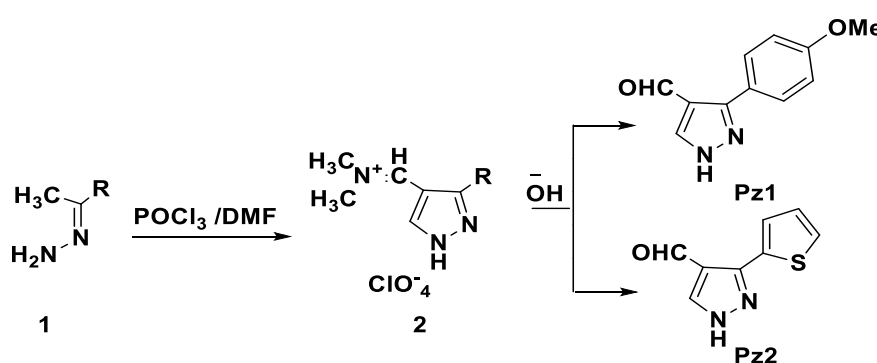


**Figure 1.** Preparation of pyrazole aldehyde derivatives.

Each aldehyde was added in an equimolar amount to the aforementioned solution.

#### 2.5. Preparation of chitosan-Schiff-base derivatives

0.1 mole of chitosan was dissolved in 1% acetic acid. Each prepared aldehyde was added in an equimolar amount to the above solution. The reaction mixture was stirred for 6 h at room temperature. This reaction mixture was poured onto ethanol, boiled and then left overnight to obtain the chitosan-Schiff base derivatives as solid products. This preparation is represented in Scheme 2 (See **Figure 2**).

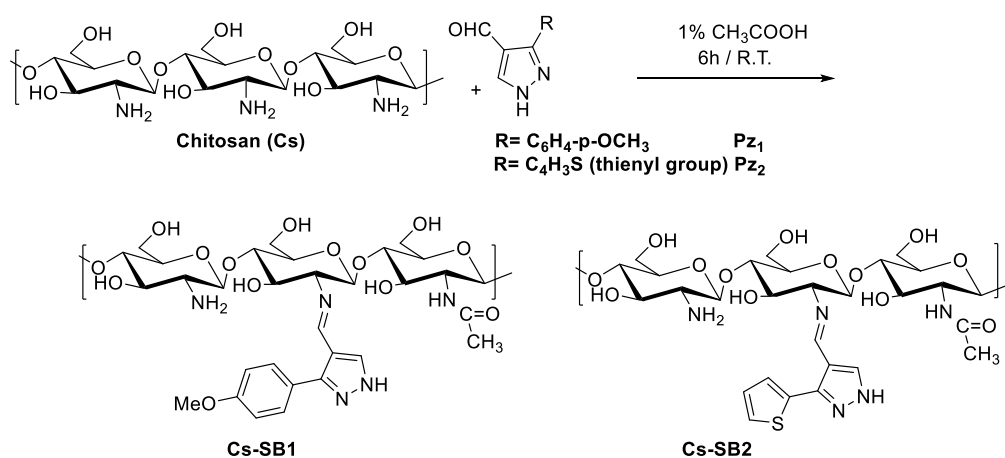


**Figure 2.** Preparation of the two chitosan-Schiff base derivatives.

## 2.6. Adsorption of Cu(II) metal ions using a batch method adjusting pH level

Adsorption of copper metal ions was performed by applying the batch adsorption experiments [39]. 20 mL of  $\text{CuCl}_2 \cdot 2\text{H}_2\text{O}$  solution with a concentration of  $5 \times 10^{-3}$  mol/L was placed in an Erlenmeyer flask to obtain a solution of pH 7. There are two other solutions of  $\text{CuCl}_2$  with pH 4 and 9 were prepared by using acetic acid/sodium acetate ( $\text{AcOH}/\text{NaOAc}$ ) and  $\text{NH}_4\text{OH}/\text{NH}_4\text{Cl}$  buffer solutions to adjust the pH level for studying the metal ions uptake at both acidic and alkaline mediums, respectively. Various adsorbent masses, 0.05, 0.10, 0.15 and 0.20 g were used and added and the adsorption equilibrium was attained after 60 min at 25 °C. The formed phases were separated by centrifugation (6000 rpm), and the amount of Cu(II) ions uptake from the solution was calculated by applying the following relationship (Equation (1)):

$$R\% = (C_0 - C_t/C_0) \times 100 \quad (1)$$

where ( $R\%$ ) is the removal efficiency;  $C_0$  = Initial concentration of Cu(II) ions in the solution;  $C_t$ : The equilibrium of Cu(II) ions.

## 2.7. Antimicrobial activity

Antibacterial activity of the tested samples was evaluated using a modified Kirby-Bauer disc diffusion method [40]. Briefly, 100 mL of the microorganisms were grown in 10 mL of fresh media until they reached a count of approximately 108 cells/mL for microorganisms [41]. 100 mL of microbial suspension were spread onto agar plates corresponding to the broth in which they were maintained. Isolated colonies of each organism, that might be playing a pathogenic role, should be selected from primary agar plates. They were examined for susceptibility by the disc diffusion method [42,43]. Of the many media available, the National Committee of Clinical Laboratory Standards (NCCLS) recommended Mueller-Hinton agar due to its good results in batch-to-batch reproducibility. Antibacterial activity of the prepared hydrogels was investigated against three types of Gram +ve bacteria (*Staphylococcus aureus* and *Bacillus Subtilis*) and three Gram -ve bacteria (*Streptococcus faecalis* and *Escherichia coli*) and Fungus (*Candida albicans*). Plates are inoculated with microorganism at 35–37 °C for 24–48 h [40]. Standard discs of Ampicillin (Antibacterial agent) and Amphotericin B (Antimicrobial agent) have served as positive controls for antibacterial activity but filter discs impregnated with 10 mL of solvent (distilled water, chloroform, DMSO) have been used as negative controls. The agar used is Mueller-Hinton agar that is rigorously tested for composition and pH. Further, the depth of the agar in the plate is considered to be a factor in the disc diffusion method. This method is well documented and standard inhibition zones have been determined for susceptible and resistant values. Blank paper discs (Schleicher and Schuell, Spain) with a diameter of 8.0 mm were impregnated with 10 mL of the tested concentration of the stock solutions. When a filter paper disc, impregnated with a tested chemical is placed on agar, the chemical will diffuse from the disc into the agar. This diffusion will place the chemical on the agar only around the disc. The size of the area of chemical infiltration around the

disc was determined by the solubility of the chemical and its molecular size. If an organism is placed on the agar, it will not grow around the disc if it is susceptible to the chemical. This area of no growth around the disc is known as a “clear zone” for the disc diffusion, the zone diameters were measured with slipping calipers of the NCCLS [41]. Agar-based methods such as E-test and disc diffusion are considered to be good alternatives because they are simpler and faster than broth-based methods [44,45].

### **3. Results and discussion**

#### **3.1. Chemistry**

Hydrazine hydrate reacted separately with 4-methoxy acetophenone and acetyl thiophene and the obtained derivatives were used to prepare 3-(4-methoxyphenyl)-4-methelene-1H-pyrazole Pz1 and 4-methelene-3-(thiophen-2-yl)-1H-pyrazole with codes Pz2, respectively, as described previously in experimental section. These aldehydes reacted with chitosan under the above-mentioned conditions to obtain two chitosan-Schiff bases Cs-SB1 and Cs-SB2. The chemical structure of both aldehydes and chitosan-Schiff bases was confirmed via FTIR spectroscopy. Thermal stability of the chitosan-Schiff bases was determined via thermogravimetric analysis. The prepared chitosan-Schiff bases products Cs-SB1 and Cs-SB2 were utilized to test the performance of adsorption of Cu (II) ions in aqueous solutions.

#### **3.2. Characterization of pyrazole aldehydes and their chitosan-Schiff bases**

The IR of the prepared pyrazole aldehydes Pz1 and Pz2 as well as their chitosan-Schiff base derivatives Cs-SB1 and Cs-SB2 are represented in **Figure 3** and are agree well with their chemical structures. For pyrazole aldehyde derivatives, Pz1 and Pz2, the appeared IR bands at 3250 and 3245  $\text{cm}^{-1}$  are related to the vibration stretching of their NH groups and the peaks at 3010 and 3101  $\text{cm}^{-1}$  assigned the CH of the two pyrazoles respectively. The aliphatic CH vibration stretching of both pyrazoles is represented by the IR peaks at 2781 and 2923  $\text{cm}^{-1}$ . The IR bands of carbonyl group, C=O, of the two pyrazoles aldehydes have appeared at 1702  $\text{cm}^{-1}$ . For Pz1, the IR peak that appeared at 1597  $\text{cm}^{-1}$  is for C=N and the other one at 1463  $\text{cm}^{-1}$  assigned to the aromatic C=C groups of pyrazole ring while these two groups are characterized by the two IR peaks at 1578 and 1462  $\text{cm}^{-1}$  for Pz2. The thiophene moiety as side chain of the pyrazole aldehyde Pz2 is represented by the presence of the IR bands at 840 and 707  $\text{cm}^{-1}$  which may be related to both C-S and C-S-C groups. The two chitosan-Schiff bases derivatives, Cs-SB1 and Cs-SB2 are characterized by their IR spectral data and represented in **Figure 3**. The two overlapping functional groups, NH and OH are characterized by the IR stretching vibration band at 3430  $\text{cm}^{-1}$ . Changes in the IR spectrum is observed by the formation of imine groups,  $\text{-N=CH-}$  in the chemical structure of the two prepared chitosan-Schiff bases (Pz1 and Pz2) and are confirmed by the presence of two IR peaks at 1637 and 1625  $\text{cm}^{-1}$  which is accompanied by the disappearance of the C=O aldehydic groups. This can easily confirm the formation of the Schiff base

derivatives.

The IR spectral data of the prepared derivative, Cs-SB1 in addition to its copper metal chelate is represented by **Figure 4**. It is clearly noticed that a slight shift for the IR band at  $1637\text{ cm}^{-1}$  that assigned the  $\text{-N=CH}$  group to  $1592\text{ cm}^{-1}$  due to the chelation process with the copper metal. This is supported by the development of the apparent IR peaks at  $419$  and  $458\text{ cm}^{-1}$  due to the formed  $\text{-N-Cu}$  linkage.

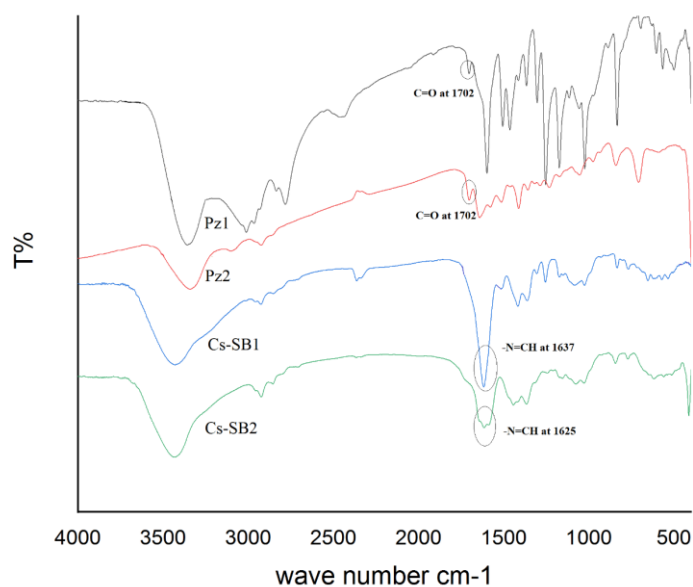


**Figure 3.** IR of two prepared pyrazoles Pz1 and Pz2 and their chitosan-Schiff bases.

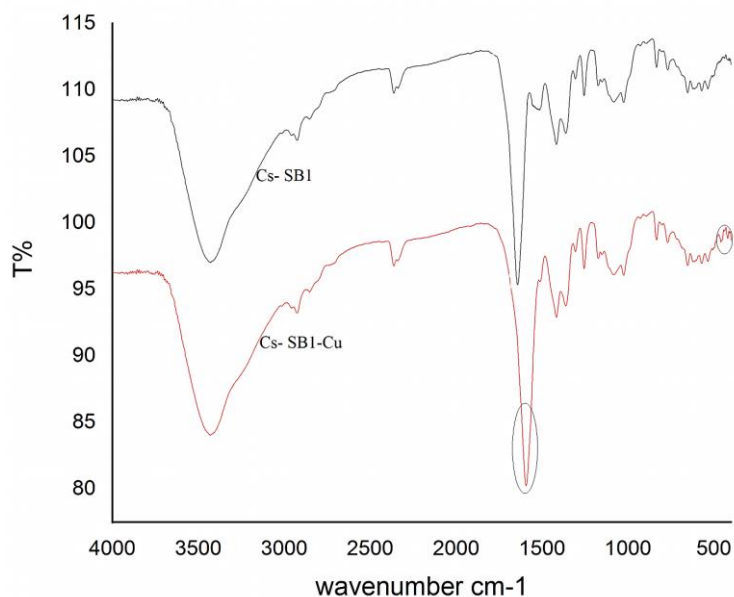


**Figure 4.** IR of Cs-SB1 and its copper metal ion chelate.

### 3.3. Thermogravimetric analysis (TGA)

Thermogravimetric analysis of chitosan in addition to its corresponding two Schiff bases Cs-SB1 and Cs-SB2 were performed for the films in an inert atmosphere within the range of  $50$  and  $800\text{ }^{\circ}\text{C}$ , with three-time repetitions, and are

displayed in **Figure 5**. TGA curves show that the first degradation step of Cs occurs in the range of 105–175 °C with a weight loss % of 6.5%. This loss in weight at the beginning of decomposition is caused by the release of water molecules from chitosan and this is followed by a slow degradation rate to record a weight loss of 11.5% at 200 °C. The second stage of degradation of chitosan begins at 225 to 370 °C at which it loses 35% of its weight. This weight loss may be related to the degradation of polymeric chains of chitosan. The last stage of decomposition is drastic and starts nearly at 400–600 °C is corresponding to the cracking of pyranose rings. The weight loss at these higher degradation temperatures 400, 500 and 600 are 37.4, 73.7 and 82.8 respectively. For the two chitosan-Schiff bases, it is observed that there is a difference in both the starting decomposition temperatures and the rate of degradation other than chitosan. The onset decomposition temperature of both Cs-SB1 and Cs-SB2 is 221 and 172 °C respectively. The Cs-SB1 showed weight loss of 6.3 and 32.7% at 300 and 400 °C whereas Cs-SB2 had weight loss of 14.5% and 34.7% at the same temperatures. At elevated temperatures, 500 and 600 °C, the weight loss % of the two Schiff bases reached 58.4 and 76.4 for Cs-SB1 and 61.6 and 80.8 for Cs-SB2 respectively.

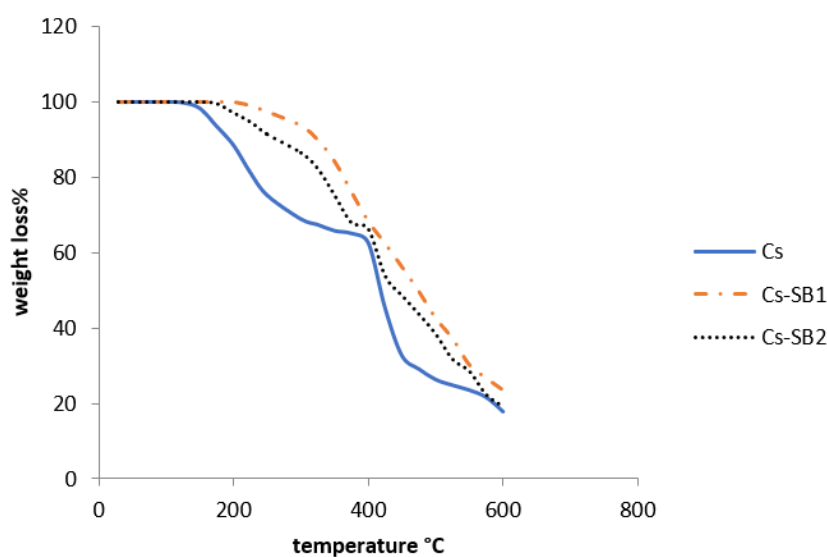
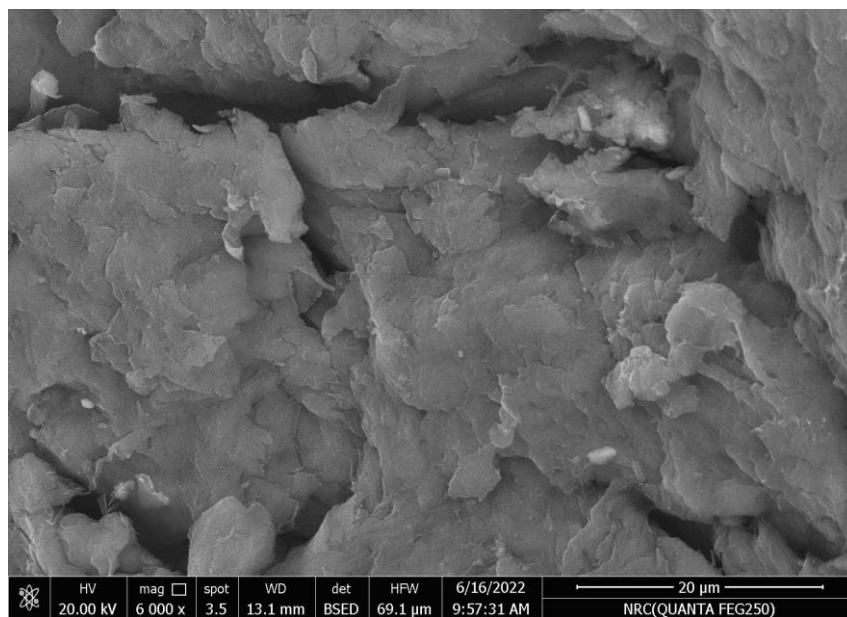


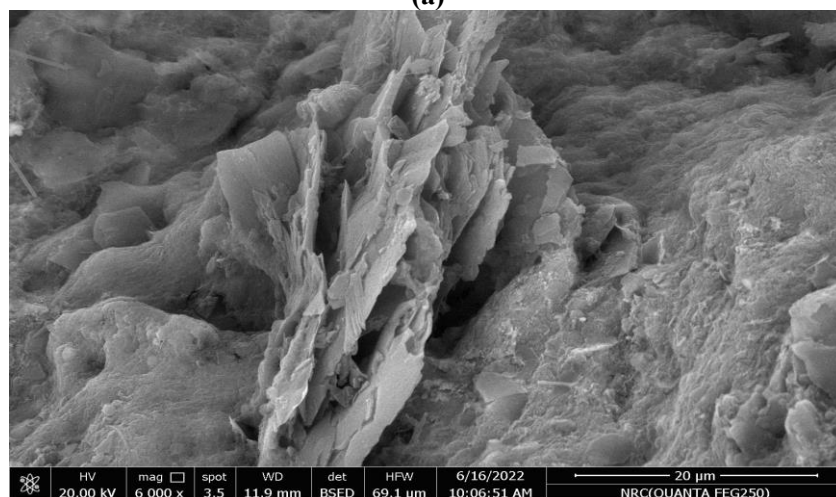
**Figure 5.** TGA of Cs and its Schiff bases, Cs-SB1 and Cs-SB2.

### 3.4. Scanning electron microscopy

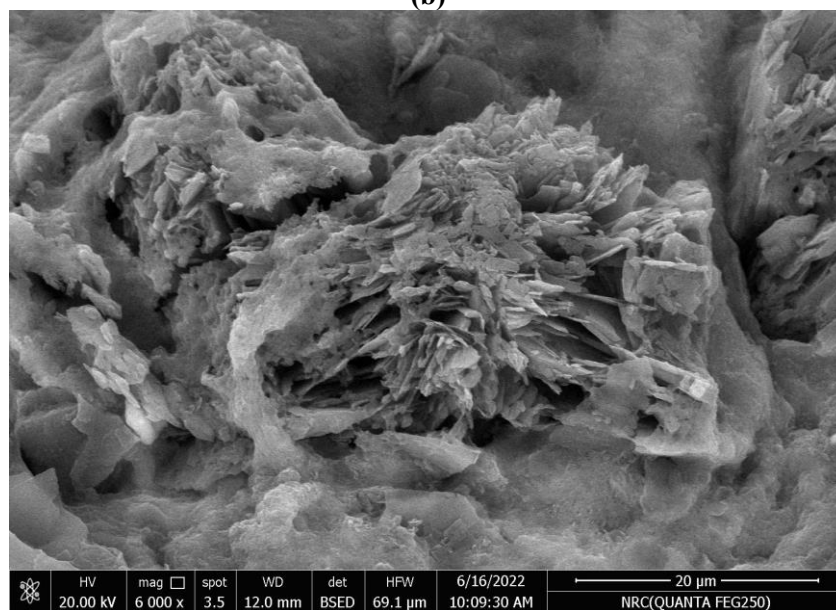
Morphological investigation of control chitosan Cs, its two Schiff bases, Cs-SB1 and Cs-SB2 in addition to their metal-adsorbed samples at different applied pH of the reaction (ranging from 4 to 9) was performed using a scanning electron microscope. As shown in **Figure 6**, the SEM image of Cs displays a relatively nonporous smooth surface. Again, in **Figure 6**, it is observed that some surface changes occurred for both Cs-SB1 and Cs-SB2 samples since they seem to have surface roughness and pores. This was a confirmation on the performed coupling of the chitosan amino group with the given pyrazole aldehydes to afford the two Schiff bases.



(a)



(b)



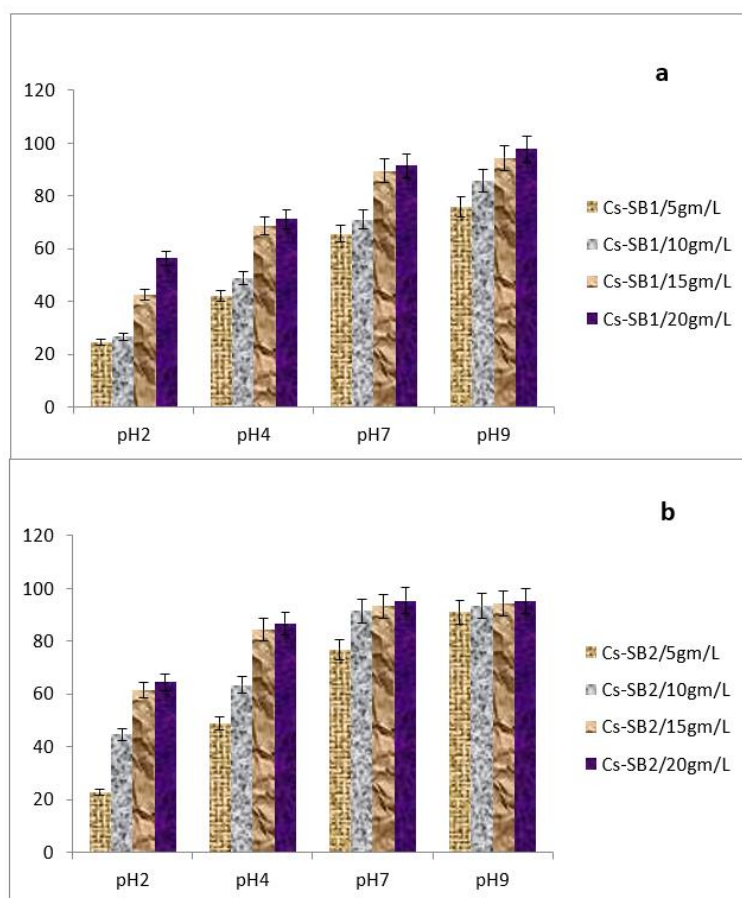
(c)

Figure 6. SEM of (a) Cs; (b) Cs-SB1; (c) Cs-SB2.

### 3.5. Cu(II) adsorption studies using a batch method

#### 3.5.1. Effect of pH on metal ions adsorption

Two chitosan-Schiff bases, Cs-SB1 and Cs-SB2 were prepared and used as adsorbent substrates for Cu(II) ions in aqueous solution using the batch adsorption method. This study concerns the effect of the pH of the applied medium, the adsorbent mass, well as its chemical structure on the efficiency of metal removal. The applied pHs were 2, 4, 7 and 9 whereas the adsorbent masses were 5, 10, 15 and 20 g/L. **Figure 7a,b** shows how these factors affect the Cu(II) removal from the aqueous solution by both Cs-SB1 and Cs-SB2. It is noticed that the metal ion removal efficacy ( $R\%$ ) has increased as the pH increases from 2 to 9 at different concentrations of the applied adsorbent [46]. The first adsorbent Cs-SB1, clearly shows that there is an increase of metal ion uptake on increasing both pH and adsorbent mass. On using adsorbent mass amounts of 0.05, 0.1, 1.5 and 2.0 g/L, the detected % of metal ion uptake at pH 2 is 24.4, 26.6 42.4 and 56.3 while at pH 4 it reached 42.1%, 48.8%, 68.7% and 70.1% respectively. However, the  $R\%$  of metal ions uptake, at pH 7, recorded 65.6%, 71%, 89.3% and 90.5%. The percentages of Cu(II) metal ion removal, at pH 9, on using this adsorbent (Cs-SB1) with the aforementioned masses reached 75.8, 85.8, 94.2, and 95.1 respectively. Therefore, it could be concluded that there was no significant increase in the removal of metal ions from the aqueous solution when the mass amount of adsorbent increased from 1.5 g/L to 2.0 g/L. The second prepared chitosan-Schiff base, Cs-SB2, shows a small increase in the adsorption of metal ions when using the same mass amounts of adsorbent and the results behave in the same trend. The removal percentages of Cu(II) ions using Cs-SB2 were detected as follows: at pH 2, the metal ions uptake is 22.8, 44.6, 61.3, and 64.3, at pH 4, these percentages are; 48.8%, 63.3%, 84.2%, and 85.6%. At pH 7, metal ions uptake was recorded at 76.67%, 91.4%, 93.1%, and 94.2%; while at pH 9, it reached 90.82%, 93.17%, 94.2%, 96.3%. As a result, the observed data showed that percentages of metal ions,  $R\%$ , are dependent on both adsorbent mass amount and the working pH. **Figure 7** shows that the increase of the adsorbent weight from 0.05 to 1.5 g/L increases metal ions uptake significantly, but after that weight the growth becomes moderate. This may be due to competition between metal ions and biosorption [47]. In other words, as the adsorbent mass increases, a lower decrease in metal ion removal is observed and this is related to sorption sites present with different affinities [48].



**Figure 7. (a) Cs-SB1; (b) Cs-SB2 for  $R\%$  removal of Cu(II) metal ions removal as a function with pH and adsorbent masses**

The effect of pH or the acidity of the medium, on the other hand, may be used to explain why Cu(II) removal increased with pH as the hydrogen ions could easily compete with the metallic ions for active sites of the adsorbent surface. So, at low pH values, the functional groups of the adsorbent were ionized and appeared in a positively charged protonated state. Electrostatic repulsion between the metal cations and these protonated groups may hinder the metal ions from adsorbing onto the surface substrate [49]. At higher pH values, the retention of metal ions becomes almost steady because small amounts of metal cations begin to deposit as hydroxides and this further supports the cation chelation on the adsorbent. The potency of investigated prepared chitosan-Schiff bases for removal of metal ions from aqueous solutions can also be explained on the basis of its chemical structure. These Schiff bases have the stable azomethine group,  $-N=CH-$ , that can coordinate with some metal ions [50,51]. The imine group of Schiff bases has a considerable role in the stabilization of the formed metal complexes since it binds the sites of some transition metals to form coordination complexes [52].

Regarding the chitosan-Schiff bases of pyrazole derivatives in this study, the working molecules contain nitrogen, oxygen (Cs-SB1) with high electronegativity enhancing the interaction between the functional group and the metal ions [53]. Cs-SB2 which has a thiophene ring with a sulfur atom adding more electronegativity for this ligand molecule, may cause higher efficiency for metal removal.

### 3.5.2. Effect of contact time on metal ions adsorption

On using the adsorbent mass amount of 20 mg/L at a pH of 9 and 25 °C, the effect of time on the metal ions adsorption was discussed. The findings are given in **Figure 8**. The results show the affinity of Cs-SB1 to adsorb the tested metal ion, Cu(II), is slightly higher than Cs-SB2. For Cs-SB1, it is obvious that the adsorption of Cu(II) ions ratio at the first 10 min showed about 29.4%, reaching higher than 96.5% during 60 min and this may be due to the more active sites for adsorption. After that time, no significant increase is shown from 70 to 90 min due to occupation of the available adsorption sites. At this stage, which is nearly at a plateau, the adsorbent's surface pores closed off and reached their maximum capacity for absorption due to the agglomeration of metal ions on the surface of the adsorbent [54].

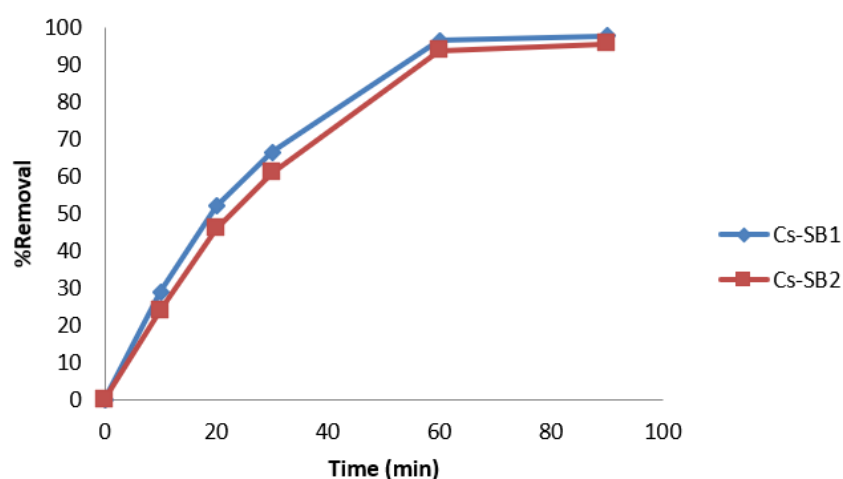


**Figure 8.** Effect of contact time of Cs-SB1 and Cs-SB2 on metal ions removal %.

### 3.5.3. Effect of temperature on metal ions adsorption

**Figure 9** shows the effect of temperature on the adsorption capacity of the two investigated chitosan Schiff bases for Cu(II) ions at a 20 mg/L concentration at pH = 9. The higher temperature was shown to significantly increase the adsorption capacity at equilibrium. The removal efficiency of copper ions adsorbed, at equilibrium, by Cs-SB1 was increased from 67.3% to 92.5% when the reaction temperature was raised from 10 to 20 °C. On the other hand, the percentages of removal efficiency of copper ions adsorbed by Cs-SB2 when the temperature was increased from 10 to 20 °C are 61.5% and 82.9%. The relative increase in the removal of the metal ions may be due to the increase of mobility of ions in solution by increasing temperature [55].

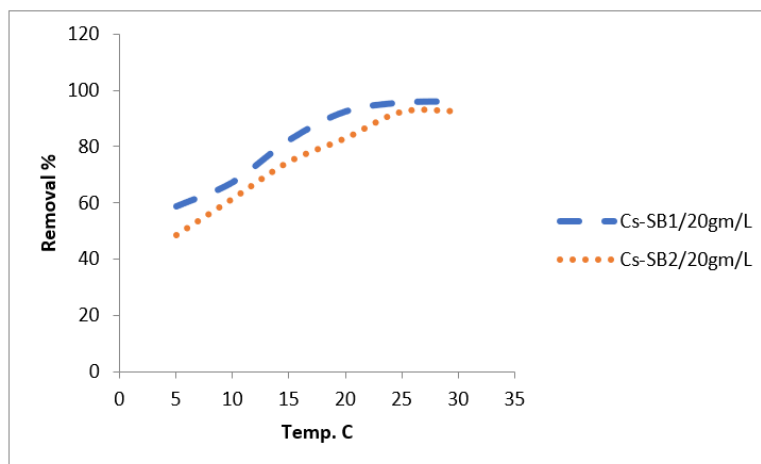
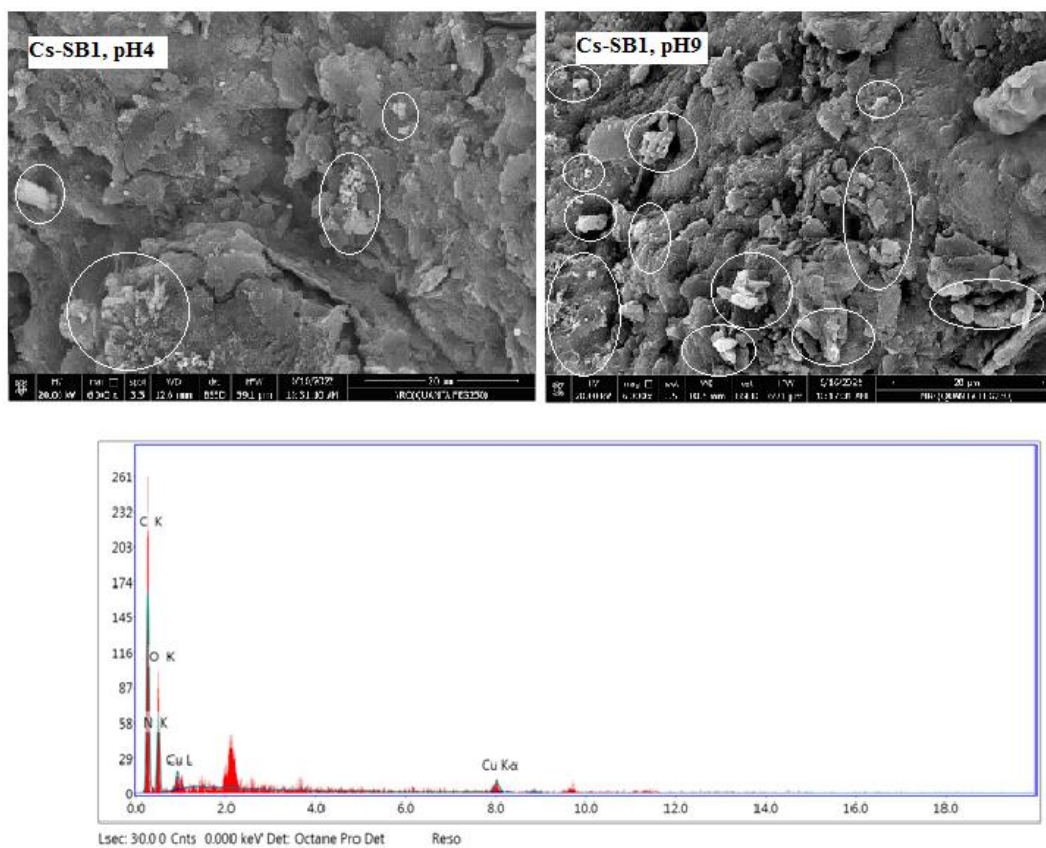


**Figure 9.** Effect of temperature on metal ions removal % by Cs-SB1 and Cs-SB2.



Element	Weight %	Atomic %	Net Int.	Error %
C K	53.25	62.4	40.36	8.75
N K	6.79	6.82	0.99	51.61
O K	33.31	29.31	16.6	15.3
CuK	6.65	1.47	4.68	22.82

**Figure 10.** SEM image of Cs-SB1/Cu(II) at pH of 4 and 9, its EDX profile and analysis of elemental constitutes in weight %.

Further explanation for the potency of the Schiff bases under study, Cs-SB1 and Cs-SB2 for Cu(II) metal ions removal from aqueous solutions is confirmed by SEM investigations and given in **Figures 10** and **11** which clarify the amount of adsorbed Cu(II) by these Schiff bases at pH values of 4 and 9 whereas the mass amount of adsorbent is 0.15 g/L via their SEM images. **Figure 10** shows the amount of adsorbed Cu(II) by Cs-SB1, which appeared in the form of spotlights, is higher at a pH of 9 with some aggregation on the surface. The EDX graph exhibited the existence of all elemental components of both the adsorbent and the adsorbed metal which gives evidence for its adsorption on the substrate surface and the characteristic peak of Cu was around 8 keV. The graph clearly shows that the chemical composition of Cs-SB1/Cu(II), at a pH of 9, in weight % (C, N, O and Cu) was recorded (53.25 wt%, 6.79 wt%, 33.31 w% and 6.65 wt% respectively).

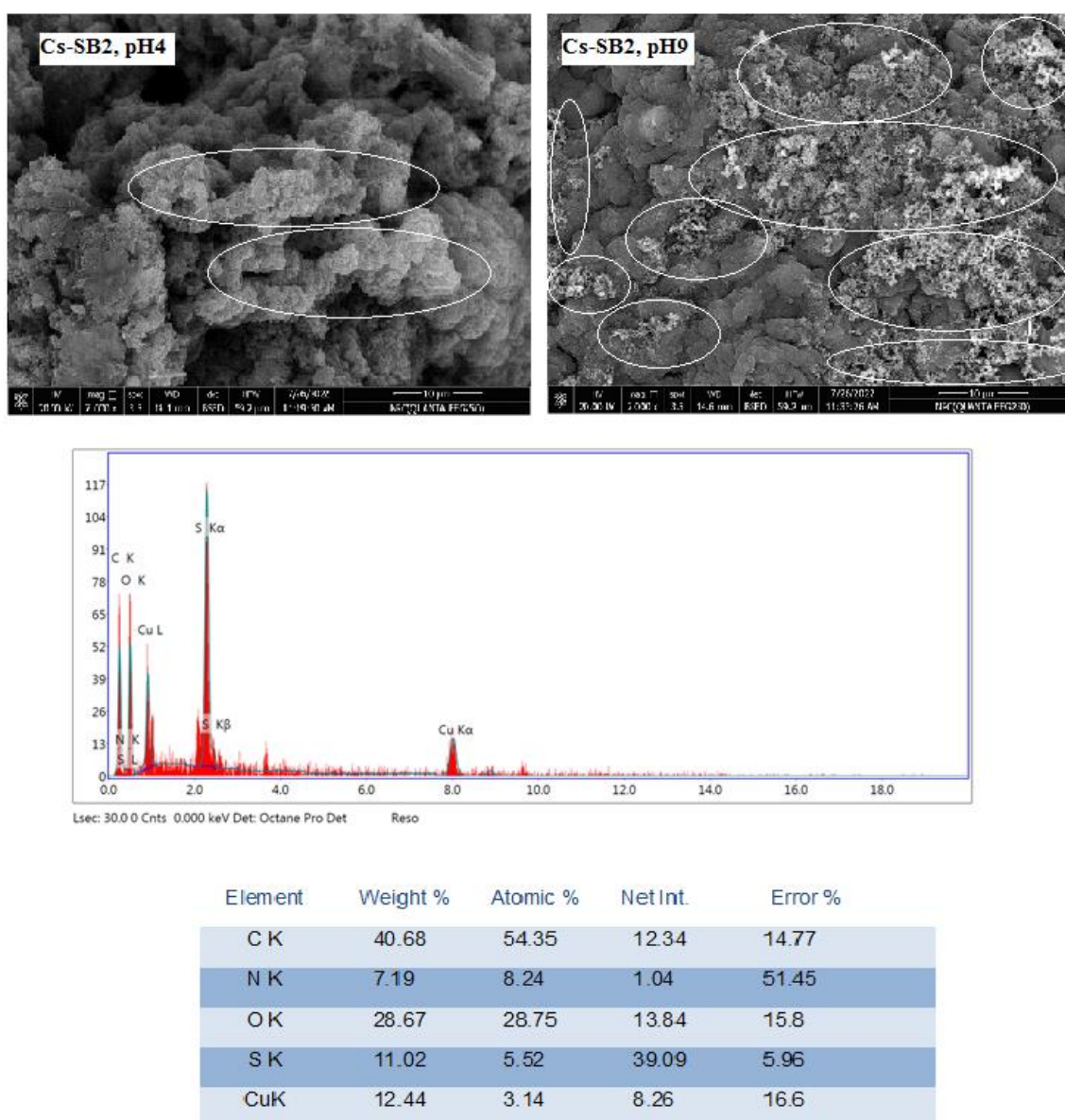


**Figure 11.** SEM image of Cs-SB2/Cu(II) at pH of 4 and 9, its EDX profile and analysis of elemental constitutes in weight %.

**Figure 11** represents the adsorption of Cu(II) by Cs-SB2 under the same

conditions and also exhibits the increase of metal ions adsorbed on the Schiff base surface at pH 9 compared to that at pH 4. EDX graph indicates that the characteristic peak of Cu appeared near 8 keV and the percentage weight of elements of the given material shows the chemical composition of Cs-SB1/Cu(II). The given chemical composition of Cs-SB1/Cu(II), at a pH of 9 with a mass amount of 0.15 g/L, in weight % (C, N, O, S, and Cu) recorded (40.68 wt%, 7.19 wt%, 28.67 wt%, 11.02% and 12.44 wt% respectively).

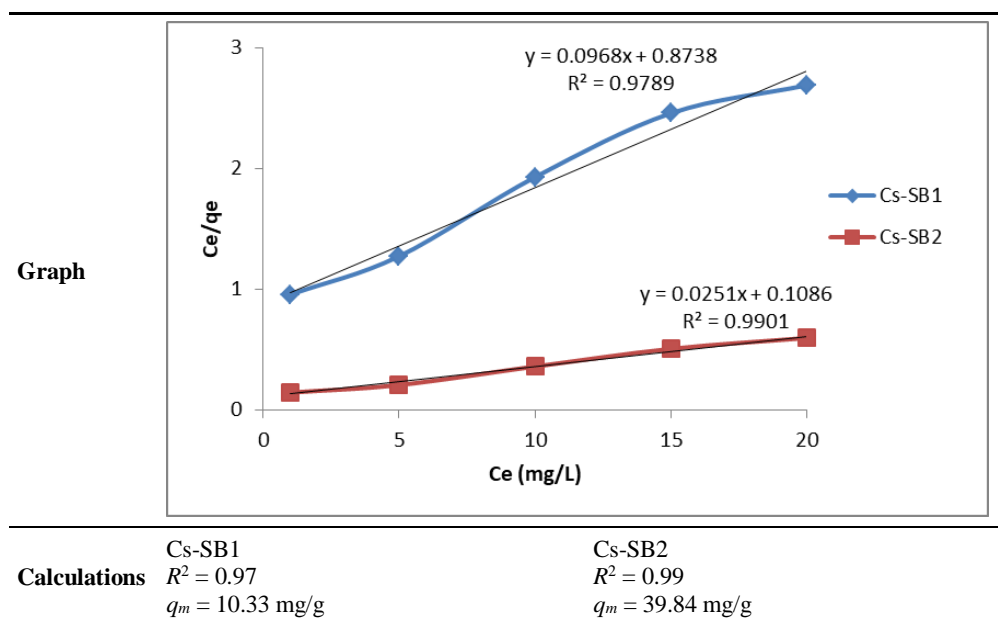
### 3.5.4. Adsorption isotherms well-suited to the adsorption of, adsorption well-fitting

Langmuir (LH) isotherm correlations showed the values of regression coefficient, ( $R^2 = 0.99, 0.96$ , respectively). The given results indicate well-fitting adsorption of Cu(II) ions on Cs-SB1 and Cs-SB2 adsorbents with LH. The determined sorption capacity ( $q_m$ ) for metal ions Cu(II) on Cs-SB1 and Cs-SB2 was calculated by using the Langmuir model (Equation (2)).

$$C_e/q_m = C_e/q_e + 1/(K_L q_e) \tag{2}$$

where ( $K_L$ ): Langmuir constants, and ( $q_m$ ): maximum adsorption capacity, ( $C_e$ ): the residual amount, and  $q_e$  the adsorption capacity at equilibrium, respectively. It was determined that maximum adsorption capacity ( $q_m$ ) = 10.33 and 39.84 mg/g, respectively) (Table 1). So, Cs-SB2 exhibited higher adsorption capacity than Cs-SB1 [56].

**Table 1.** Adsorption isotherm.



### 3.5.5. The recycle regeneration properties

The reusability of the adsorbents Cs-SB1 and Cs-SB2 was studied. For regeneration of the adsorbents, they were washed by the use of a solution of 0.1 M NaOH and the formed materials were used in cycles consequently, by repeating the regeneration/adsorption experiment for 5 cycles. It was observed that high efficiency

towards the adsorption of Cu(II) ions and accordingly, the % removal of Cu(II) ions was slightly decreased in the five cycles. This was indicated by the stability of the adsorbents (**Figure 12**).

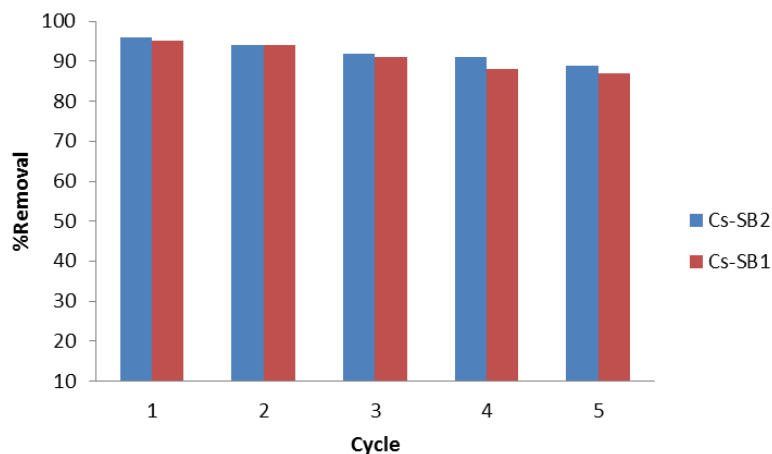


**Figure 12.** Recyclability of Cs-SB1 and Cs-SB2 adsorbents in removal of Cu(II) ions.

### 3.5.6. Antimicrobial activity of investigated compounds

The antibacterial activity of all investigated samples was carried out and **Table 2** displayed their screening data. The investigation was performed against some Gram +ve (*B. Subtittle* and *St. aurous*) as well as some other Gram –ve bacteria (*St. faecalis* and *E. coli*). Antifungal activity of the compounds under test was carried out against *C. al*

**Table 2.** Antimicrobial activity of investigated prepared compounds.

Sample	Inhibition zone diameter (mm/mg sample)				
	<i>B. Subtittle</i>	<i>St. aurous</i>	<i>St. faecalis</i>	<i>E. coli</i>	<i>C. albicans</i>
	G +ve		G –ve		Fungus
DMSO	0.0	0.0	0.0	0.0	0.0
Cs	7 ± 13	10 ± 12	8 ± 0.06	10 ± 0.11	7 ± 0.22
Pz1	11 ± 09	13 ± 15	10 ± 0.23	12 ± 0.18	8 ± 0.16
Pz2	12 ± 24	13 ± 0.09	11 ± 0.15	14 ± 0.21	10 ± 0.11
Cs-SB1	15 ± 15	17 ± 0.16	14 ± 0.26	15 ± 0.09	11 ± 0.13
Cs-SB2	18 ± 11	18 ± 0.06	17 ± 0.14	19 ± 0.12	14 ± 0.24
Cs-SB1-Cu(II)	19 ± 21	19 ± 0.17	17 ± 0.22	20 ± 0.27	15 ± 0.07
Cs-SB2-Cu(II)	19 ± 32	19 ± 0.13	18 ± 0.09	20 ± 0.14	15 ± 0.12
Ampicillin (100 µg/mL)	20 ± 0.5	18 ± 0.5	18 ± 0.6	22 ± 0.6	
Amphotericin B (100 µg/mL)					19 ± 0.27

The antimicrobial activity is represented by measuring the diameters of growth inhibition zones in mm. The given results revealed that all the tested compounds showed interesting and considerable antimicrobial activity, however, with a degree of variation. The results show that the inhibitory effects of chitosan derivatives (Cs-SB1 and Cs-SB2) are higher than those of both native chitosan and the prepared pyrazole

derivatives against all tested microorganisms with respect to the reference antibacterial and antifungal agents. The pyrazole derivative Pz2 and its chitosan-Schiff base, Cs-SB2, exhibited a significant increase in inhibitory potency compared to both Pz1 and Cs-SB1. Cs-SB2 shows antibacterial activity against both Gram +ve types of bacteria, *B. Subtitle* and *St. aurous*, to reach 90% and 100% respectively. It shows also good activity against the two tested G –ve bacteria *St. faecalis* and *E. coli* to record 94 and 86% respectively while its antifungal activity was 73.6%. All results are compared to the two antimicrobial reference drugs. Further antimicrobial evaluation was carried out for the two chitosan-Schiff bases adsorbed copper metal ion, Cs-SB1/Cu(II) and Cs-SB2/Cu(II). Both antibacterial and antifungal activity of these two samples exhibited higher efficiencies than their corresponding chitosan-Schiff bases against all tested microorganisms with no appreciable differences in their activities. **Figure 13** displays the antimicrobial efficacies of investigated compounds against the microorganisms under test in comparison with the standard antimicrobial agents. Results of antimicrobial activity of prepared pyrazoles and their chitosan-Schiff bases can be explained on the basis of their chemical structures. So, the considerable antimicrobial activity of pyrazole derivatives, Pz1 and Pz2, may be due to their well-known properties as azoles. The pyrazole nitrogen attached to the positively charged acidic hydrogen atom may interact electrostatically with the negatively charged cell membrane of the microorganism and this can prevent the microbial growth [57,58]. There is a slight observed increase in antimicrobial properties for Pz2 to Pz1, and this may be related to the thiophene moiety attached to the pyrazole ring in Pz2 with its activity against various microbial species [59,60]. The improved antimicrobial inhibitory effects of the investigated chitosan derivatives, Cs-SB1 and Cs-SB2, when compared to both chitosan and the two pyrazole aldehyde derivatives may be attributed to the presence of chitosan units and also the imine group of Schiff bases.

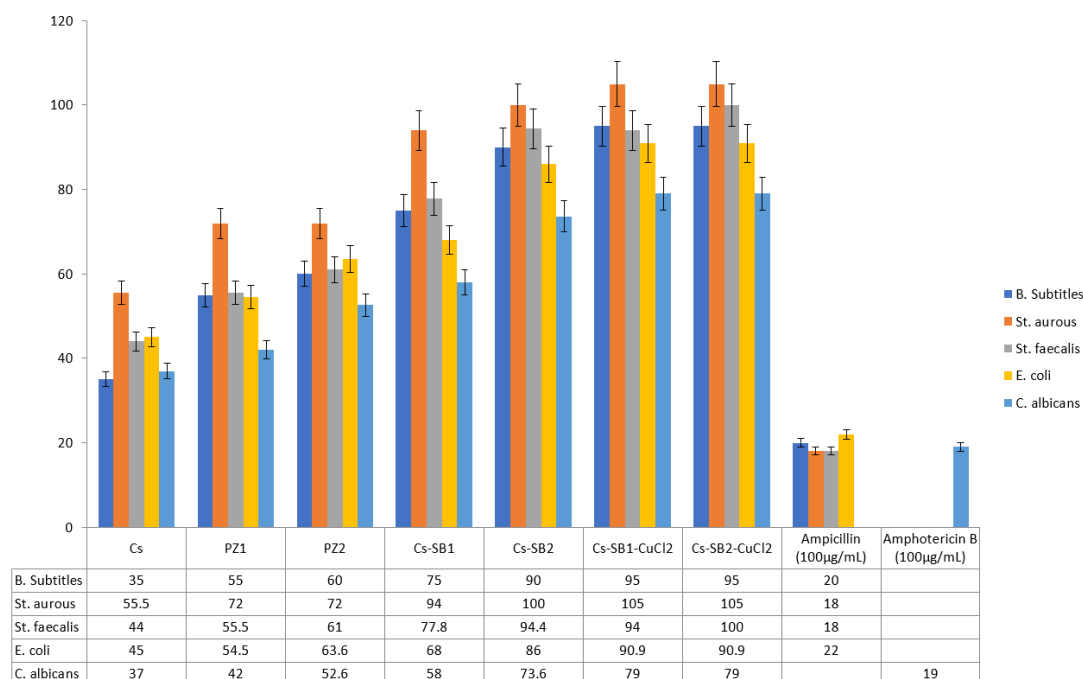


**Figure 13.** Antimicrobial efficacy of investigated compounds in comparison with the reference drug.

Previous research [61] reported that chitosan has many proposed mechanisms to explain how it affects microorganisms that vary according to the structure of the cell wall membrane of bacteria and its metabolic procedure.

The first suggested mode of action is the disruption of microbial cell walls that is caused by electrostatic force interactions between chitosan amino groups with their positive charge and the microbial cell wall that has a negative charge. The other proposed mechanism is the interaction of microbial DNA with chitosan that prevents mRNA and protein synthesis through chitosan permeating the bacterial cell and then the nuclei [62]. Finally, the presence of the Schiff base imine group,  $-\text{CH}=\text{N}$ , may be associated with the significant antibacterial activity of these utilized compounds. The presence of  $\pi$ -electrons on this imine group may boost the lipophilicity of chitosan-Schiff bases. So, this may enable the Schiff-base molecule to penetrate the microbial cell wall membrane, disrupting the respiration mechanism of the microbial cell.

So, it could be concluded that the occurrence of these disruptions in the main vital processes of microorganisms may easily prevent protein synthesis, which will impede further bacterial growth [63,64].

#### **4. Conclusion**

Preparation of two pyrazole aldehyde derivatives (Pz1 and Pz2) was performed and then they were reacted with chitosan to afford the two pyrazole-chitosan Schiff bases, 3-(4-methoxyphenyl)-4-methelene-1H-pyrazole-chitosan (Cs-SB1) and 4-methelene-3-(thiophen-2-yl)-1H-pyrazole-chitosan (Cs-SB2), respectively. These chitosan-Schiff bases were subjected to being utilized as adsorbents for Cu(II) ions removal from aqueous solutions using the batch adsorption method.

The chemical structure of prepared aldehydes and their corresponding Schiff bases was confirmed via FTIR spectroscopic analysis. Determination of thermal properties of the investigated samples using the thermogravimetric analysis technique, showed their enhanced thermal properties in terms of higher initial decomposition temperatures and lower extent of weight loss. Scanning electron microscopy (SEM) as well as energy dispersive X-ray (EDX) for the prepared Schiff bases adsorbed metal ions in different aqueous solutions were carried out. SEM images showed the changes that occurred to the surface morphology of chitosan on its reaction with the Schiff bases whereas the EDX graph confirmed the existence of these adsorbed metal ions on the surface substrate and the adsorptive efficiency of these prepared samples for Cu(II) ions. Results of the batch adsorption method also showed the good ability of the investigated Schiff bases to adsorb Cu(II) ions from aqueous solutions. The expected mechanism of copper elimination interprets because of the results of FTIR analysis that indicated the formation of N-Cu linkage on adsorbent surfaces, that it might be responsible for the adsorption of Cu(II) ions as Cu-H ion exchange or Cu(II) ion-adsorbent surface complexation, or both. Adsorption of Cu(II) metal ions onto Cs-SB1 and Cs-SB2 surfaces was best matched to the Langmuir model, proposing that Cu(II) ions adsorption was accomplished on the homogeneous surfaces with the monolayer coverage. The two samples, Cs-SB1 and Cs-SB2 had maximal adsorption capacities of 10.33 and 39.48 mg/g respectively. Antimicrobial activity of the compounds Cs, Pz1, Pz2, Cs-SB1, Cs-

SB2, Cs-SB1-Cu, Cs-SB2-Cu was carried out. Two Gram +ve bacteria (*Bacillus Subtiles* and *Staphylococcus aureus*), two Gram –ve bacteria (*Streptococcus faecalis* and *Escherichia coli*) and *Candida albicans* as fungi were used in this study. All investigated compounds showed good antimicrobial activity with varying degrees when compared to the applied standard antimicrobial agents.

**Author contributions:** Conceptualization, RAAM and YMAM; methodology, RAAM and STR; software, RAAM; validation, RAAM, STR and HAEN; formal analysis, RAAM; investigation, RAAM and STR; resources, RAAM; data curation, RAAM and STR; writing—original draft preparation, RAAM and STR; writing—review and editing, RAAM; visualization, STR; supervision, STR; project administration, RAAM and STR; funding acquisition, STR. All authors have read and agreed to the published version of the manuscript.

**Funding:** The authors acknowledge National Research Centre for the valuable support through research project fund entitled (Development of novel Poly(vinyl chloride)/carboxymethyl chitosan/ZnO nanocomposite materials for health and hospital care applications), of ID: 13020202.

**Conflict of interest:** The authors declare no conflict of interest.

## References

1. Bhargava S, Uma V. Rapid extraction of Cu(II) heavy metal from industrial waste water by using silver nanoparticles anchored with novel Schiff base. *Separation Science and Technology*. 2018; 54(7): 1182-1193. doi: 10.1080/01496395.2018.1527853
2. Wang X. Nanomaterials as Sorbents to Remove Heavy Metal Ions in Wastewater Treatment. *Journal of Environmental & Analytical Toxicology*. 2012; 02(07). doi: 10.4172/2161-0525.1000154
3. Okoya A, Akinyele A, Amuda O, et al. Chitosan-Grafted Carbon for the Sequestration of Heavy Metals in Aqueous Solution. *American Chemical Science Journal*. 2016; 11(3): 1-14. doi: 10.9734/acsj/2016/21813
4. Pohl A. Removal of Heavy Metal Ions from Water and Wastewaters by Sulfur-Containing Precipitation Agents. *Water, Air, & Soil Pollution*. 2020; 231(10). doi: 10.1007/s11270-020-04863-w
5. Hassan R, Arida H, Montasser M, et al. Synthesis of New Schiff Base from Natural Products for Remediation of Water Pollution with Heavy Metals in Industrial Areas. *Journal of Chemistry*. 2013; 2013(1). doi: 10.1155/2013/240568
6. Li M, Wang M, Zhang L, et al. Adsorption of Pd(II) ions by electrospun fibers with effective adsorption sites constructed by N, O atoms with a particular spatial configuration: Mechanism and practical applications. *Journal of Hazardous Materials*. 2023; 458: 132014. doi: 10.1016/j.jhazmat.2023.132014
7. Cheng N, Zhang L, Wang M, et al. Highly effective recovery of palladium from a spent catalyst by an acid- and oxidation-resistant electrospun fibers as a sorbent. *Chemical Engineering Journal*. 2023; 466: 143171. doi: 10.1016/j.cej.2023.143171
8. Li M, Zhang L, Wang M, et al. A nanofiber with a p- $\pi$  conjugated structure designed based on the Jahn-Teller effect for the removal of cupric tartrate from wastewater. *Journal of Colloid and Interface Science*. 2023; 650: 161-168. doi: 10.1016/j.jcis.2023.06.195
9. Hamed AA, Abdelhamid IA, Saad GR, et al. Synthesis, characterization and antimicrobial activity of a novel chitosan Schiff bases based on heterocyclic moieties. *International Journal of Biological Macromolecules*. 2020; 153: 492-501. doi: 10.1016/j.ijbiomac.2020.02.302
10. Casadidio C, Peregrina DV, Gigliobianco MR, et al. Chitin and Chitosans: Characteristics, Eco-Friendly Processes, and Applications in Cosmetic Science. *Marine Drugs*. 2019; 17(6): 369. doi: 10.3390/md17060369
11. Matica MA, Aachmann FL, Tøndervik A, et al. Chitosan as a Wound Dressing Starting Material: Antimicrobial Properties and Mode of Action. *International Journal of Molecular Sciences*. 2019; 20(23): 5889. doi: 10.3390/ijms20235889
12. Rodríguez-Rodríguez R, Espinosa-Andrews H, Velasquillo-Martínez C, et al. Composite hydrogels based on gelatin,

- chitosan and polyvinyl alcohol to biomedical applications: a review. *International Journal of Polymeric Materials and Polymeric Biomaterials*. 2019; 69(1): 1-20. doi: 10.1080/00914037.2019.1581780
13. Molnár Á. The use of chitosan-based metal catalysts in organic transformations. *Coordination Chemistry Reviews*. 2019; 388: 126-171. doi: 10.1016/j.ccr.2019.02.018
  14. Tang X, Huang T, Zhang S, et al. The role of sulfonated chitosan-based flocculant in the treatment of hematite wastewater containing heavy metals. *Colloids and Surfaces A: Physicochemical and Engineering Aspects*. 2020; 585: 124070. doi: 10.1016/j.colsurfa.2019.124070
  15. Syeda SEZ, Khan MS, Skwierawska AM. Chitosan-based modalities with multifunctional attributes for adsorptive mitigation of hazardous metal contaminants from wastewater. *Desalination and Water Treatment*. 2024; 320: 100679. doi: 10.1016/j.dwt.2024.100679
  16. Vunain E, Mishra A, Mamba B. Dendrimers, mesoporous silicas and chitosan-based nanosorbents for the removal of heavy-metal ions: A review. *International Journal of Biological Macromolecules*. 2016; 86: 570-586. doi: 10.1016/j.ijbiomac.2016.02.005
  17. Maleki A, Pajootan E, Hayati B. Ethyl acrylate grafted chitosan for heavy metal removal from wastewater: Equilibrium, kinetic and thermodynamic studies. *Journal of the Taiwan Institute of Chemical Engineers*. 2015; 51: 127-134. doi: 10.1016/j.jtice.2015.01.004
  18. Rocha LS, Almeida Â, Nunes C, et al. Simple and effective chitosan based films for the removal of Hg from waters: Equilibrium, kinetic and ionic competition. *Chemical Engineering Journal*. 2016; 300: 217-229. doi: 10.1016/j.cej.2016.04.054
  19. Shukla SK, Mishra AK, Arotiba OA, et al. Chitosan-based nanomaterials: A state-of-the-art review. *International Journal of Biological Macromolecules*. 2013; 59: 46-58. doi: 10.1016/j.ijbiomac.2013.04.043
  20. Shaalan N, Abdulwahhab S. Synthesis, characterization and biological activity study of some new metal complexes with Schiff's bases derived from [O-vanillin] with [2-amino-5-(2-hydroxy-phenyl)-1,3,4-thiadiazole]. *Egyptian Journal of Chemistry*. 2021. doi: 10.21608/ejchem.2021.66235.3432
  21. Pervaiz M, Quratulain R, Ejaz A, et al. Thiosemicarbazides, 1,3,4 thiadiazole Schiff base derivatives of transition metal complexes as antimicrobial agents. *Inorganic Chemistry Communications*. 2024; 160: 111856. doi: 10.1016/j.inoche.2023.111856
  22. Neelufar, Rangaswamy J, Ankali KN, et al. The Mn(II), Co(II), Ni(II) and Cu(II) complexes of (Z)-N'((1H-indol-3-yl)methylene)nicotinohydrazide Schiff base: synthesis, characterization and biological evaluation. *Journal of the Iranian Chemical Society*. 2022; 19(9): 3993-4004. doi: 10.1007/s13738-022-02580-1
  23. Singh A, Gogoi HP, Barman P, et al. Novel thioether Schiff base transition metal complexes: Design, synthesis, characterization, molecular docking, computational, biological and catalytic studies. *Applied Organometallic Chemistry*. 2022; 36(6). doi: 10.1002/aoc.6673
  24. Keypour H, Rezaeivala M, Valencia L, et al. Synthesis and characterization of some new Co(II) and Cd(II) macrocyclic Schiff-base complexes containing piperazine moiety. *Polyhedron*. 2009; 28(17): 3755-3758. doi: 10.1016/j.poly.2009.08.021
  25. Barbosa HFG, Attjioui M, Ferreira APG, et al. New series of metal complexes by amphiphilic biopolymeric Schiff bases from modified chitosans: Preparation, characterization and effect of molecular weight on its biological applications. *International Journal of Biological Macromolecules*. 2020; 145: 417-428. doi: 10.1016/j.ijbiomac.2019.12.153
  26. Wang W, Wu G, Zhu T, et al. Synthesis of -thiazole Schiff base modified SBA-15 mesoporous silica for selective Pb(II) adsorption. *Journal of the Taiwan Institute of Chemical Engineers*. 2021; 125: 349-359. doi: 10.1016/j.jtice.2021.06.004
  27. Zhao J, Luan L, Li Z, et al. The adsorption property and mechanism for Hg(II) and Ag(I) by Schiff base functionalized magnetic Fe<sub>3</sub>O<sub>4</sub> from aqueous solution. *Journal of Alloys and Compounds*. 2020; 825: 154051. doi: 10.1016/j.jallcom.2020.154051
  28. Janeta M, Lis T, Szafert S. Zinc Imine Polyhedral Oligomeric Silsesquioxane as a Quattro-Site Catalyst for the Synthesis of Cyclic Carbonates from Epoxides and Low-Pressure CO<sub>2</sub>. *Chemistry – A European Journal*. 2020; 26(60): 13686-13697. doi: 10.1002/chem.202002996
  29. Malekshah RE, Shakeri F, Khaleghian A, et al. Developing a biopolymeric chitosan supported Schiff-base and Cu(II), Ni(II) and Zn(II) complexes and biological evaluation as pro-drug. *International Journal of Biological Macromolecules*. 2020; 152: 846-861. doi: 10.1016/j.ijbiomac.2020.02.245
  30. Sharef HY, Fakhre NA. Rapid adsorption of some heavy metals using extracted chitosan anchored with new aldehyde to

- form a schiff base. *PLOS ONE*. 2022; 17(9): e0274123. doi: 10.1371/journal.pone.0274123
31. Zalloum HM, Al-Qodah Z, Mubarak MS. Copper Adsorption on Chitosan-Derived Schiff Bases. *Journal of Macromolecular Science, Part A*. 2008; 46(1): 46-57. doi: 10.1080/10601320802515225
  32. Kong M, Chen XG, Xing K, et al. Antimicrobial properties of chitosan and mode of action: A state of the art review. *International Journal of Food Microbiology*. 2010; 144(1): 51-63. doi: 10.1016/j.ijfoodmicro.2010.09.012
  33. Monier M. Adsorption of Hg<sup>2+</sup>, Cu<sup>2+</sup> and Zn<sup>2+</sup> ions from aqueous solution using formaldehyde cross-linked modified chitosan–thioglyceraldehyde Schiff's base. *International Journal of Biological Macromolecules*. 2012; 50(3): 773-781. doi: 10.1016/j.ijbiomac.2011.11.026
  34. Anush SM, Vishalakshi B, Kalluraya B, et al. Synthesis of pyrazole-based Schiff bases of Chitosan: Evaluation of antimicrobial activity. *International Journal of Biological Macromolecules*. 2018; 119: 446-452. doi: 10.1016/j.ijbiomac.2018.07.129
  35. Badgujar JR, More DH, Meshram JS. Synthesis, Antimicrobial and Antioxidant Activity of Pyrazole Based Sulfonamide Derivatives. *Indian Journal of Microbiology*. 2017; 58(1): 93-99. doi: 10.1007/s12088-017-0689-6
  36. Hassan S. Synthesis, Antibacterial and Antifungal Activity of Some New Pyrazoline and Pyrazole Derivatives. *Molecules*. 2013; 18(3): 2683-2711. doi: 10.3390/molecules18032683
  37. Satheesha Rai N, Kalluraya B, Lingappa B, et al. Convenient access to 1,3,4-trisubstituted pyrazoles carrying 5-nitrothiophene moiety via 1,3-dipolar cycloaddition of sydnone with acetylenic ketones and their antimicrobial evaluation. *European Journal of Medicinal Chemistry*. 2008; 43(8): 1715-1720. doi: 10.1016/j.ejmech.2007.08.002
  38. Kira MA, Abdel-Rahman MO, Gadalla KZ. The vilsmeier-haack reaction - III Cyclization of hydrazones to pyrazoles. *Tetra Lett*. 1969; 10(2): 109-110. doi: 10.1016/S0040-4039(01)88217-4
  39. Abdel-Wahab BF, Khidre RE, Farahat AA. Pyrazole-3(4)-carbaldehyde: synthesis, reactions and biological activity. *Zhdankin VV, ed. Arkivoc*. 2011; 2011(1): 196-245. doi: 10.3998/ark.5550190.0012.103
  40. Kosa SA, Al-Zhrani G, Abdel Salam M. Removal of heavy metals from aqueous solutions by multi-walled carbon nanotubes modified with 8-hydroxyquinoline. *Chemical Engineering Journal*. 2012; 181-182: 159-168. doi: 10.1016/j.cej.2011.11.044
  41. Jeong JH, Shin KS, Lee JW, et al. Analysis of a novel class I integron containing metallo-β-lactamase gene VIM-2 in *Pseudomonas aeruginosa*. *The Journal of Microbiology*. 2009; 47(6): 753-759. doi: 10.1007/s12275-008-0272-2
  42. Kanokwiroon K, Teanpaisan R, Wititsuwannakul D, et al. Antimicrobial activity of a protein purified from the latex of *Hevea brasiliensis* on oral microorganisms. *Mycoses*. 2008; 51(4): 301-307. doi: 10.1111/j.1439-0507.2008.01490.x
  43. National Committee for Clinical Laboratory Standards. Reference method for Broth Dilution Antifungal susceptibility testing of *Conidium-Forming Filamentous Fungi*: proposed guideline M38-A. NCCLS, Wayne, PA, USA; 2002.
  44. National Committee for Clinical Laboratory Standards. Method for antifungal disk diffusion susceptibility testing of yeast: proposed guideline M44-P. NCCLS, Wayne, PA, USA; 2003.
  45. Liebowitz LD, Ashbee HR, Evans EGV, et al. Two-year global evaluation of the susceptibility of *Candida* species to fluconazole by disk diffusion. *Diagn Microbiol Infect Dis*. 2001; 40(1-2): 27-33. doi: 10.1016/s0732-8893(01)00243-7
  46. Matar MJ, Ostrosky-Zeichner L, Paetznick VL, et al. Correlation between E-Test, Disk Diffusion, and Microdilution Methods for Antifungal Susceptibility Testing of Fluconazole and Voriconazole. *Antimicrobial Agents and Chemotherapy*. 2003; 47(5): 1647-1651. doi: 10.1128/aac.47.5.1647-1651.2003
  47. Mahmoud RK, Mohamed F, Gaber E, et al. Insights into the Synergistic Removal of Copper(II), Cadmium(II), and Chromium(III) Ions Using Modified Chitosan Based on Schiff Bases-g-poly(acrylonitrile). *ACS Omega*. 2022; 7(46): 42012-42026. doi: 10.1021/acsomega.2c03809
  48. Cieslak Golonka M. Toxic and mutagenic effects of chromium (VI). A review. *Polyhedron*. 1996; 15(21): 3667–3918. doi: 10.1016/0277-5387(96)00141-6
  49. Ho YS, Huang CT, Huang HW. Equilibrium sorption isotherm for metal ions on tree fern. *Process Biochemistry*, 2002; 37(12): 1421-1430. doi: 10.1016/S0032-9592(02)00036-5
  50. Monier M, Ayad DM, Wei Y, et al. Preparation and characterization of magnetic chelating resin based on chitosan for adsorption of Cu(II), Co(II), and Ni(II) ions. *Reactive and Functional Polymers*. 2010; 70(4): 257-266. doi: 10.1016/j.reactfunctpolym.2010.01.002
  51. Undegaonkar MG, Sinkar SN, Bhosale VN, et al. Solvent Free Synthesis and Characterization of Few Metal Complexes of Schiff Base Derived from 2-Amino-5, 6-dimethyl Benzimidazole and Syringaldehyde. *International Journal of Pharmaceutical Sciences and Drug Research*. 2020; 13(03): 240-245. doi: 10.25004/ijpsdr.2021.130301

52. Ahmed MO, Shripip A, Mansoor M. Synthesis and Characterization of New Schiff Base/Thiol-Functionalized Mesoporous Silica: An Efficient Sorbent for the Removal of Pb(II) from Aqueous Solutions. *Processes*. 2020; 8(2): 246. doi: 10.3390/pr8020246
53. Zhang Z, Song Q, Jin Y, et al. Advances in Schiff Base and Its Coating on Metal Biomaterials—A Review. *Metals*. 2023; 13(2): 386. doi: 10.3390/met13020386
54. Mustapha S, Shuaib DT, Ndamitso MM, et al. Adsorption isotherm, kinetic and thermodynamic studies for the removal of Pb(II), Cd(II), Zn(II) and Cu(II) ions from aqueous solutions using Albizia lebbeck pods. *Applied Water Science*. 2019; 9(6). doi: 10.1007/s13201-019-1021-x
55. Mafu LD, Mamba BB, Msagati TAM. Synthesis and characterization of ion imprinted polymeric adsorbents for the selective recognition and removal of arsenic and selenium in wastewater samples. *Journal of Saudi Chemical Society*. 2016; 20(5): 594-605. doi: 10.1016/j.jscs.2014.12.008
56. Hanaor DAH, Ghadiri M, Chrzanowski W, et al. Scalable Surface Area Characterization by Electrokinetic Analysis of Complex Anion Adsorption. *arXiv*. Published online 2021. doi: 10.48550/ARXIV.2106.03411
57. Khalil AM, Abdel-Monem RA, Darwesh OM, et al. Synthesis, Characterization, and Evaluation of Antimicrobial Activities of Chitosan and Carboxymethyl Chitosan Schiff-Base/Silver Nanoparticles. *Journal of Chemistry*. 2017; 2017: 1-11. doi: 10.1155/2017/1434320
58. Peng XM, Cai GX, Zhou CH. Recent Developments in Azole Compounds as Antibacterial and Antifungal Agents. *Current Topics in Medicinal Chemistry*. 2013; 13(16): 1963-2010. doi: 10.2174/15680266113139990125
59. Mabkhot Y, Alatibi F, El-Sayed N, et al. Synthesis and Structure-Activity Relationship of Some New Thiophene-Based Heterocycles as Potential Antimicrobial Agents. *Molecules*. 2016; 21(8): 1036. doi: 10.3390/molecules21081036
60. Mabkhot YN, Kaal NA, Alterary S, et al. Antimicrobial activity of thiophene derivatives derived from ethyl (E)-5-(3-(dimethylamino)acryloyl)-4-methyl-2-(phenylamino)thiophene-3-carboxylate. *Chemistry Central Journal*. 2017; 11(1). doi: 10.1186/s13065-017-0307-z
61. Tamer TM, Hassan MA, Omer AM, et al. Synthesis, characterization and antimicrobial evaluation of two aromatic chitosan Schiff base derivatives. *Process Biochemistry*. 2016; 51(10): 1721-1730. doi: 10.1016/j.procbio.2016.08.002
62. Haj NQ, Mohammed MO, Mohammed LE. Synthesis and Biological Evaluation of Three New Chitosan Schiff Base Derivatives. *ACS Omega*. 2020; 5(23): 13948-13954. doi: 10.1021/acsomega.0c01342
63. Webster A, Halling MD, Grant DM. Metal complexation of chitosan and its glutaraldehyde cross-linked derivative. *Carbohydrate Research*. 2007; 342(9): 1189-1201. doi: 10.1016/j.carres.2007.03.008
64. Abdel-Monem RA, Khalil AM, Darwesh OM, et al. Antibacterial properties of carboxymethyl chitosan Schiff-base nanocomposites loaded with silver nanoparticles. *Journal of Macromolecular Science, Part A*. 2019; 57(2): 145-155. doi: 10.1080/10601325.2019.1674666